Self-consistent Simulations of Interactions between Spacecraft and Plumes of Electric Thrusters

IEPC-2013-73

Presented at the 33rd International Electric Propulsion Conference,

The George Washington University • Washington D.C. • USA

October 6 - 10, 2013

Matias Wartelski[1] and Christophe Theroude[2]

Astrium Satellites, Toulouse, 31000, France

Carlos Ardura[3]

Sogeti High Tech for Astrium Satellites, Toulouse, 31000 France

And

Eric Gengembre[4]

ESA-ESTEC, Noordwijk, 2201, The Netherlands

Abstract: The Spacecraft Plasma Interaction System (SPIS) tool, initially developed to model interactions between environmental plasma and spacecraft, has been extended in order to model interactions between spacecraft and plasma plumes of electric thrusters. In a first step, plume models for the SPT-100, PPS-1350G, T5, T6, RIT4, RIT10, RIT22, HEMP3050, Indium and Cesium FEEP thrusters were implemented in SPIS. These models were then tuned and validated using public experimental data. In a second step, a specific ground test was conducted with the µN-RIT thruster. The neutraliser behaviour was observed to be strongly influenced by its coupling to the chamber and therefore to the spacecraft once in orbit: a simple method was developed to take this phenomenon into account in SPIS charging simulations. In the final step, SPIS was used to perform self-consistent simulations of plume-spacecraft interactions at system level. A model developed with SPIS could reproduce qualitatively the effect on SMART-1 potential of daily solar array rotation. Moreover, this model allows studying the effect on solar cells coverglass potentials.

I. Introduction and Overview of the AISEPS Project

ASTRIUM has 10 years of Electric Propulsion (EP) flight experience and 15 years of experience in EP-SC interaction analyses with own-developed simulation tools. The interaction between SpaceCraft (SC) and the ion/electron cloud exhausted by thrusters –the so-called plume- is a key issue of EP accommodation. Plume-

[1] Electric Propulsion Engineer, Electric Propulsion Group, matias.wartelski@astrium.eads.net.

[2] Space Physics Modelling Team Leader, christophe.theroude@astrium.eads.net.

[3] Space Physics Engineer, Space Physics Group, ext.zxmulsoge068@astrium.eads.net.

[4] Technical Officer, Electric Propulsion Section, eric.gengembre@esa.int.

induced erosion, contamination, electric potential transients, dynamic effects, thruster electromagnetic self-emission and disturbance by plume of RF signal propagation are the main plume-related effects. Space industry is currently observing an increasing interest for Electric Propulsion (EP) and its implementation on both scientific and telecommunications missions. This leads to increasing needs of EP-SC interactions analyses of new configurations to help architecture trade-off as well as detailed design.

In this context, it was necessary for Astrium to complement its set of simulation tools with a more sophisticated and detailed simulation tool. The AISEPS study, funded by the European Space Agency (ESA), thus aimed at:

- gaining more understanding on SC-EP plume interactions, in particular plume forming and SC charging;
- gathering available experimental plume data into a common electronic database;
- consolidating plume modelling methods developed in Europe in the past 10 years;
- implementing plume models in SPIS in order to model self-consistently plume forming, SC charging and therefor plume-SC interactions like erosion and contamination. This simulation approach, explained in §II, is a good compromise between modelling accuracy and simulation required resources.

The project resulted from the collaboration of different organisations. FOTEC gathered, in an electronic plume database, experimental and model plume data for the following electric thrusters: SPT-100, PPS-1350G & -5000, RIT4, 10 & 22, HEMP3050, T5 & 6, In and Cs-FEEP. FOTEC also specified plume models for these thrusters. Astrium implemented the models in SPIS and tuned them by comparing simulation to experimental results from the database. Plume models are briefly described in §II.A.

The µN-RIT was fired by Astrium Lampoldshausen and the University of Gieβen in the Corona vacuum chamber at ESTEC with a specific test setup: plume measurements were taken at different thrust levels, for different cathode configurations and at different levels of background pressure. Astrium Satellites used this fresh data to challenge the SPIS ability to simulate plume behaviour under different system conditions. The successful validation of SPIS is briefly presented in §II.B.

Finally, Astrium Satellites could simulate SMART1 absolute and differential charging during plasma thruster firing and for different solar panel orientations. Thanks to specific developments performed by ONERA on the SPIS code, the models take into account the arrangement of solar cell arrays, whose interconnectors (ICs) are known to play a key role on SC charging. The modelling approach and obtained results are described in §III.

II. Plume Models Validation and System Tool

A. Plume Models Description and Validation

A summary of plume models implementation and validation is presented hereafter and more detail can be found in [1]. The plume modelling approach chosen in the frame of AISEPS has been widely used in industry in the past years because it provides a very good comprise between accuracy and time & computer resources consumption. It is based on hybrid PIC simulations.

In this approach, both high and low-energy plume ions, so-called primary and Charge-EXchange (CEX), are modelled with the Particle-In-Cell (PIC) method. High energy ions and slow neutral atoms are injected at the thruster exit plane, which is represented in the simulation as a boundary surface. Low-energy ions are produced in the simulation volume by charge-exchange collisions between primary ions and neutrals (those coming from the thruster or from residual gas in vacuum

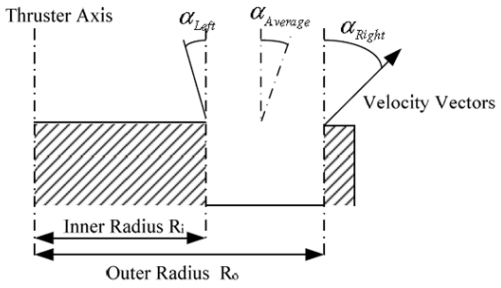

Figure 1: HET plume model boundary conditions.

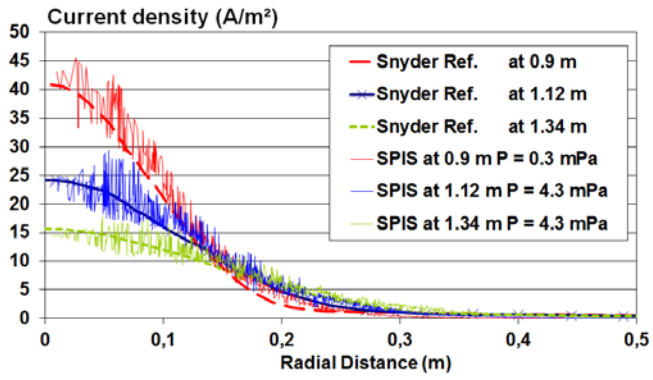

Figure 2: Measured vs simulated T6 current density.

chambers). The injection conditions in terms of density, energy and angle are specific to each thruster: Figure 1 shows the typical form of injection conditions for a Hall Effect Thruster (HET). Boundary conditions at the injection surface are tuned for each thruster so that the obtained plume profile in the far field – distance to thruster higher than 0.5 m- matches experimental data. Thus, plume models are partly phenomenological.

Concerning plasma potential, electron density and temperature, the implemented models offer different options: either assuming that electron and ion densities are equal and calculating the potential with a barometric law (Boltzmann-type) or solving the Poisson equation to get the potential and calculating the electron density with a barometric law (Boltzmann-type). In both cases, one can choose constant or variable electrons temperature and used barometric laws are consistent with these choices.

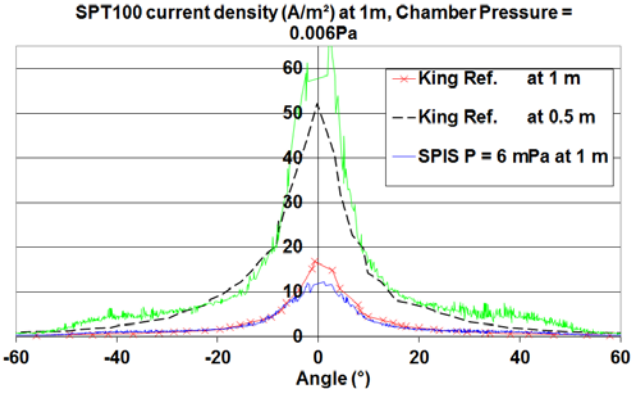

Figure 3: Measured vs simulated SPT-100 current density.

Due to the complexity of the involved physics and to the time and computer constraints within industrial projects, the models do not include a number of physical phenomena. Indeed, thruster discharge channel is not simulated and is supposed to be represented by the injection conditions at the boundary surface. Magnetic field is neither included in the current model because its effect is weak in the far field; however, for near field studies, it may appear interesting to take it into account in future improvements of the model. In terms of collisions, only charge exchange, which is the dominant phenomenon for interactions with satellites, are modelled.

Figure 2 and Figure 3 compare, for two thrusters, simulated and measured plume data. The linear scale allows verifying that the correlation in the main plume beam is very good.

Figure 4 and Figure 5 compare, this time, simulated and measured data in log scale, which allows focusing the comparison on current density at large angles, where CEX ions are dominant. The correlation in this region, which is more difficult to simulate, is satisfactory. An effort is currently being performed in order to obtain even better plume models for HET-type thrusters: improved plume models without the bump at 40-60° and better fitting of experimental data at large angles are currently under development.

At the end of this study phase, all plume models except that of PPS5000 had been tuned and validated mainly in terms of far-field current density. The models fit very well experimental data in the main beam region; in the backflow region (high angles with regard to plume axis), the models predict current densities in the same order of magnitude that experimental data, which is very satisfactory because experimental data in this region have a lot of uncertainty due to pollution by vacuum chamber.

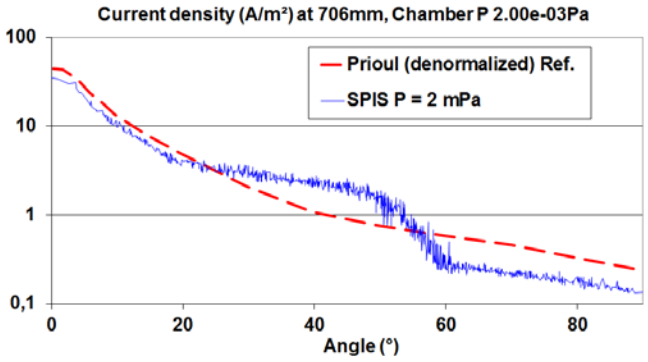

Figure 4: Measured vs simulated PPS-1350G current density.

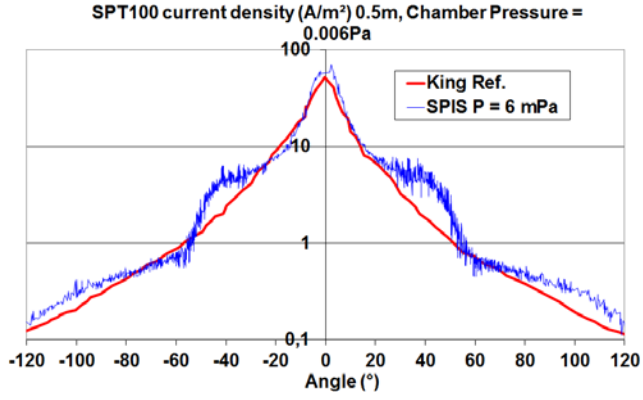

Figure 5: Measured vs simulated SPT-100 current density.

B. **System Tool**

In order to prove the ability of the developed tool to make predictions at system level, a dedicated test was performed in the Corona chamber of the Electric Propulsion Laboratory at ESTEC. The test setup and results were presented in a dedicated paper [2] and the validation of the system tool using these results was presented in a separate paper [3]. Thus, this second phase of the study is also presented briefly hereafter.

A 37-hole prototype of the µN-RIT thruster was built by the University of Gießen and, together with a filament used as neutraliser, placed in the Corona chamber as shown in Figure 6.

A sketch of the plume diagnostics setup, which includes Faraday cups and 3 kV and 300 V Retarding Potential Analysers (RPA) is shown in Figure 7.

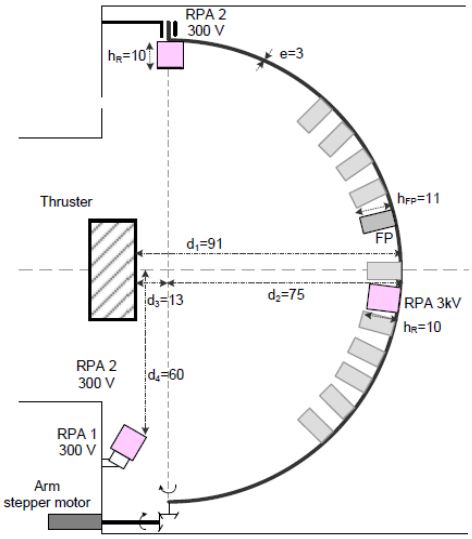

Figure 7: Plume diagnostics setup.

between the chamber structure and the ground of the power supply system and neutraliser.

Figure 8 shows that current density predicted by SPIS at different background pressures matches measured data except for angles between 20 and 40 degrees, which correspond to the transition from main beam –composed of high energy ions- and backflow region –composed of low energy ions. The modelling of this transition zone needs to be improved.

The measured characteristic I-V curve of the µN-RIT neutraliser (emitted current vs coupling potential) for different test conditions is plotted in Figure 9. The curve in vacuum is obtained by extrapolation (see Figure 10).

As shown in Figure 9, the test provided the following lessons concerning neutraliser behaviour:

- In floating configuration, the neutraliser can always fully neutralise the ion beam by adjusting its potential with regard to the chamber (called coupling potential).
- When grounded, the neutraliser, unable

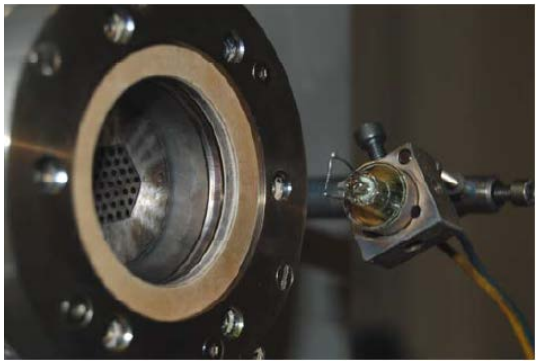

Figure 6: µN-RIT and filament.

The thruster, cathode and plume behaviour were monitored for a number of different operation configurations: 3 different levels of thrust - 100, 250 and 500 µN-, four levels of imposed background pressure in the vacuum chamber - 2e-7, 1.2e-6, 3e-6, 6e-6 mbar- and two different electrical couplings –grounded and floating-

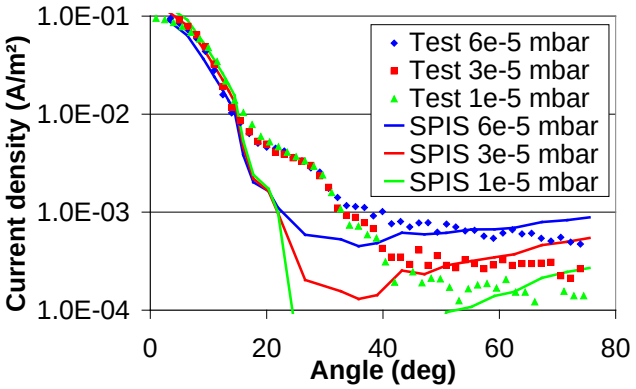

Figure 8: µN-RIT test - SPIS vs test data at 500 µN.

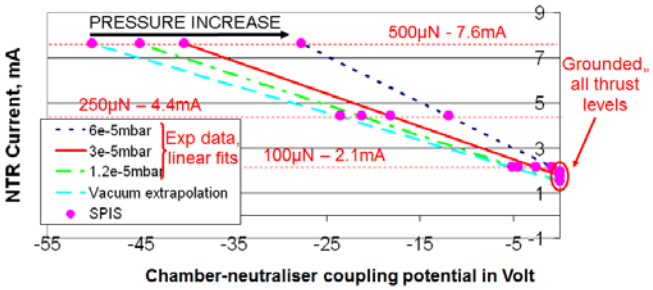

Figure 9: Measured I-V curve of the µN-RIT neutraliser.

to adjust the coupling potential (always equal to 0 V) can never fully neutralise the ion beam: the electron current is limited to 2 mA approximately.

- In floating configuration, for a given background pressure, the absolute value of the coupling potential for which the neutraliser electron current equals thruster ion current, increases linearly when the electron current increases.
- In floating configuration, for a given thrust/ion current level, the absolute value of the coupling potential for which the neutraliser electron current equals thruster ion current decreases when the background pressure increases.

The observations mentioned above are discussed in [3] and are not the object of this paper.

V in the I-V curves is the potential of the neutraliser with regard to the ground structure (potential reference in ground measurements). These I-V curves can be assumed to remain true in space simply by defining V as the potential of the neutraliser with regard to infinity (potential reference in space). This assumption, based on SMART-1's flight experience, was justified in [3] and is discussed in §III.A.

Measured I-V curves were thus extrapolated to vacuum, then specified in SPIS. Hence, this tool can be used to predict SC charging and neutraliser behaviour in space for different electric couplings. This approach is sketched in Figure 11. The SC simplified electric circuit in SPIS takes into account the electric thruster ion beam and the electron current emitted by the neutraliser according to the specified I-V curve ($f(V_{NTR})$ in Figure 11).

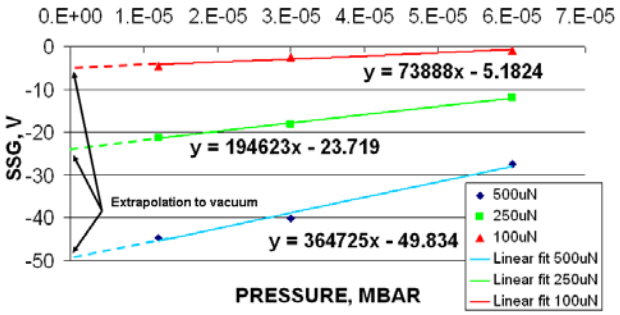

Figure 10: Extrapolation to vacuum of I-V curves.

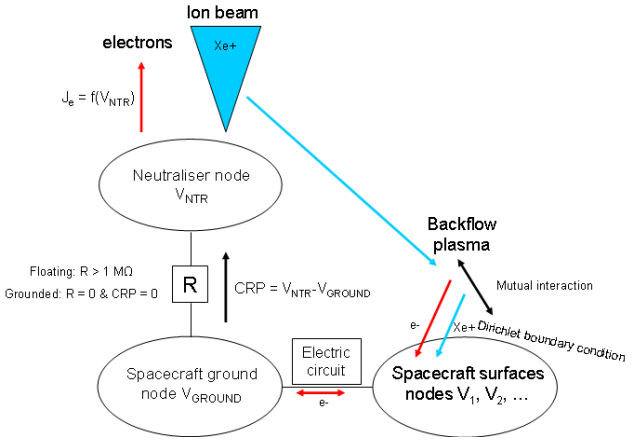

Figure 11: Sketch of SC electric circuit with electric thruster and neutraliser.

III. Self-Consistent Simulations of the SMART-1 Spacecraft

A. SMART-1 Return of Experience

SMART-1 (2003-2006) was the first European mission which implemented a Hall Effect Thruster. The electric propulsion subsystem –based on the PPS-1350G thruster- flight experience is presented and discussed in many papers like [4], [5] [6] and [7]. Some lessons of interest for our paper are listed hereafter:

- According to [7], in flight, in steady state and excluding beginning of life, the absolute potential (with respect to infinity) of the cathode was equal to the cathode coupling potential measured on ground (with respect to the chamber structure): -18.5 V. Guessing this result before the flight was not obvious.
- This justifies extrapolation to space conditions of neutraliser I-V curves measured on ground.
- This also means that measurement of the so-called Cathode Reference Potential (CRP) –potential of the cathode with respect to SC ground– provides an indirect in-situ measurement of SC absolute potential:

$$V_{SC} = -18.5\ V - CRP$$

The constant -18.5 V is valid for SMART-1 cathodes and, using on-ground measurement, should be adjusted for each specific thruster.

- CRP daily oscillations –with amplitude of ~6 V- were correlated to Solar Array (SA) rotation. The same phenomenon is observed in Astrium's fleet. The consensus within the plasma community (see [5] and [7]) is that solar cell InterConnectors (IC) with positive potentials drain large electron currents

from the plasma plume. These currents contribute and drive the overall electrical equilibrium between the plasma plume, space plasma and SC. Rotation of the SA leads to modification of electron current drained by IC, which are mainly on one side of the solar panel, and hence modify the SC absolute potential. This effect was reproduced with more or less sophisticated models (see [5] and [7]).

B. Modelling approach and parameters

The AISEPS study aimed firstly at reaching with SPIS at least the same level of prediction capability than other models developed in Europe during the first years of electric propulsion experience. Secondly, it aimed at extending the prediction capability by using pre-existing capacities of SPIS. Indeed, SPIS is the most advanced European tool for simulation of SC-plasma interactions: on one side, the tool simulates environment plasma taking into account SC as a boundary condition; on the other side, it computes absolute and differential SC charging taking into account many different interaction phenomena with the plasma at its surfaces. This permits self-consistent simulations of plasma and SC charging.

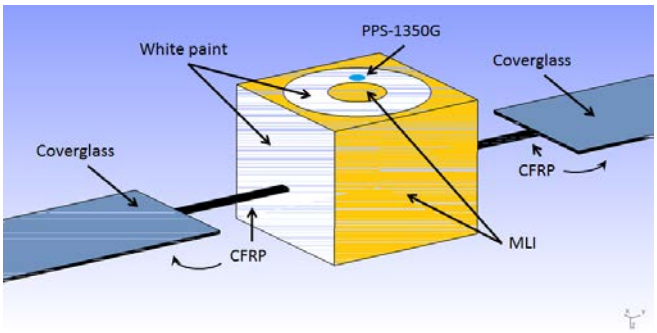

Figure 12: Geometrical model of SMART-1.

Figure 12 shows the SMART-1 geometrical model and coatings used in SPIS simulations. The plume is modelled with the PPS-1350G model tuned and validated during the first phase of the study (see §II.A and [1] for more detail).

The SMART-1 electrical architecture was such that the EP power supply and cathode were electrically decoupled from the SC ground. Hence, the cathode fully guarantees electrical balance between the EP subsystem and space by fully neutralising the ion beam, i.e. the net current between the EPS and space can be assumed to be 0. Thus, in steady state the net leak current between the SC ground and the EPS is also 0. Absolute cathode potential is -18.5 V as explained in §A. In brief, there is no need to simulate neutraliser behaviour in this configuration because it does not affect the overall SC charging.

The absolute potential of the SC ground is left floating. The coatings considered as conductors have the same potential as the SC ground, while the dielectric potentials can develop both a surface and bulk differential potential.

At this stage, in order to simplify the problem, it is considered that plume plasma dominates interactions with SC so that environment plasma is not modelled. Nor secondary and photo-electron emission are simulated.

In order to better split and understand diverse mechanisms of plasma-SA interactions, the SA model has been enriched progressively from the simplest model, named 1, to the more sophisticated model, named 6 (see Table 1).

	1	2	3	4	5	6
Solar panels	1 panel out of 6		All 6 panels: 3 per side			
SA angles	0, 180	0, 45, 90, 180	0, 45, 180	0, 180	0	
IC geometrical model	Physical surface exposed to plasma.	No physical surface: see model 2 description.		No physical surface: see model 4 description.		
IC potential	V_{ground}+50V everywhere			Linear variation from V_{ground} to V_{ground}+55V over each solar cell string section		
SA mesh	Coarse: ~200mm				Refined: 50mm	
IC collection ratio	N/A	Model A (see Figure 13)				Model B (see Figure 13)

Table 1: SMART-1 solar array models.

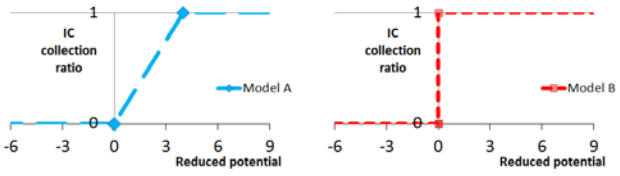

Figure 13: ICs' collection ratio models.

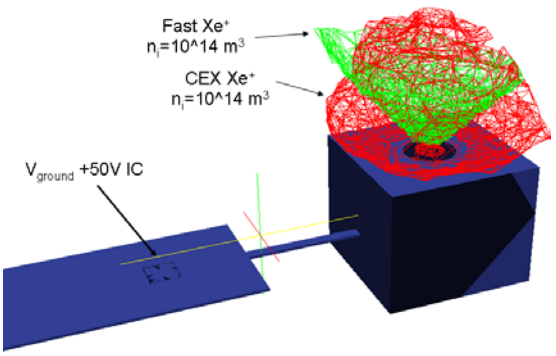

Figure 14: View of model 1.

C. Model Discussion and Results

Model 1 description: Model 1 is very simple (see Figure 14): in order to reduce computer and time resources, only 1 out of 6 solar panels is represented and only ICs with the most positive potential (V_{ground}+50 V) are represented because at first order they drive SC potential. Geometrically, ICs are modelled as one single rectangular surface of area equal to the total area of real ICs with potential V_{ground}+50 V. It is considered that the ICs surface is in direct interaction with plume plasma, so the Orbit Motion Limited (OML) model is used to calculate the total electron current collected by the IC:

$$J_e = J_{e0} \cdot e^{e|\Phi_{IC}|/kT_e} \text{ when } \Phi_{IC}<0 \text{ repelled}$$

$$J_e = J_{e0} \cdot (1 + e\Phi_{IC} / kT_e) \text{ when } \Phi_{IC}>0 \text{ attracted}$$

where $J_{e0} = -eN_e\,(kT_e / 2\pi m_e)$ is the ambient electron current outside the IC's sheath.

Model 1 results: In spite of the simplicity of model 1, Figure 15 shows that, like [5] and [7], it is able to reproduce the effect on SC potential of SA rotation during thruster operation: the ground potential is -35 V at equilibrium when the solar cells are facing the plume and -18 V when the panel is turned 180°.

However, the amplitude of this potential excursion, at least 17 V, is very high compared to the daily excursion of around 6 V observed in flight. This is the precise symptom that the effect of ICs on SC charging is overestimated in model 1 because they are collecting too many electrons. This conducts us to improve modelling of solar cell-plasma interactions.

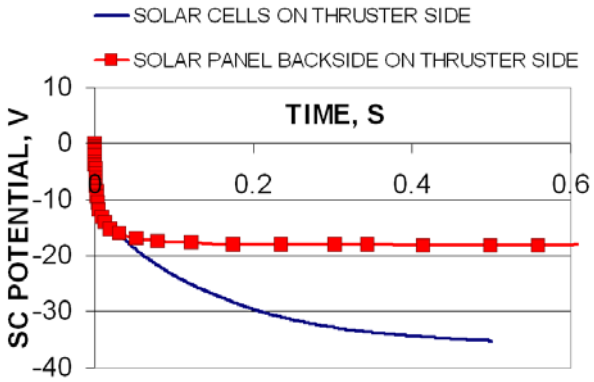

Figure 15: Model-1-predicted ground's potential vs time for two SA angles.

Model 2 description: The first limit of model 1 is that all ICs have been represented as a unique rectangular surface per panel: SPIS would not support a real geometrical representation of IC in a system level simulation.

To sort out this problem, ONERA DESP has implemented "implicit" IC modelling. Instead of being represented by geometrical forms in the 3D model, the user just specifies, over any rectangular surface, an analytical distribution of ICs, in terms of potential evolution and surface ratio. For example, one can specify that over a solar panel, ICs represent 5 % of the total surface and their potential grows linearly between V_{ground} and V_{ground}+100 V along the panel. The IC, which are many and small, are considered to be spread uniformly over the panel. SMART-1's model 2 takes advantage of this new approach and ICs appear no longer in the geometrical model.

Another important limit of model 1 and [5] is that they assume undisturbed plume plasma to reach and interact with ICs, so that ICs drain large amounts of electrons from this source. In reality, ICs are very small and thin metallic corpses located in between solar cells, whose external surface is made of coverglass, a dielectric material. Electron dynamics in the IC's vicinity are certainly complex and depend on ICs' and coverglass' potentials, geometries and on electron energy. These parameters influence the amount of electrons collected by ICs and the amount collected by coverglass. This phenomenon is taken into account in [7] by tuning the distribution of electron current between ICs and coverglass until SMART-1's absolute potential matches in-flight data.

The approach here is similar: in the absence of a precise analytical description of electron dynamics around the ICs, and in the absence of dedicated experimental data, a simple parametric model, yet different from [7], is proposed and tuned in order to match SMART-1's in-flight data. Yet simple, this model has the advantage of helping us simulate and understand complex charging mechanisms.

The model assumes that the undisturbed plume plasma flowing towards the solar panels only sees a coverglass surface. On one side, plume plasma is simulated taking coverglass potential as a boundary condition and the OML model is used to calculate the total electron and ion currents crossing the coverglass sheath as a function of coverglass potential. However, the particularity of the model here, developed by ONERA DESP, is that the electron and ion currents are not fully collected by the coverglass surface itself. Indeed, ICs are considered to be fully inside the plasma sheath developed over the coverglass surface, which is equivalent to say

that coverglass potential fully shields ICs' potentials. But unlike outside the sheath, the sheath inside is not populated by quasi-neutral plasma. Thus, ICs' potentials are not shielded and can thus potentially attract ions and electrons. In fine, if we take electrons for example, ICs collect between 0 and 100% of the OML current crossing the coverglass sheath and coverglass the rest of it.

A simple model has been implemented in SPIS by ONERA to evaluate the distribution of currents between ICs and coverglass: the model assumes that, for a particle with energy E and charge q having reached the panel at a position where the coverglass local potential is Φ_{DIEL} and the IC's local potential is Φ_{IC}, the probability of being collected by the local IC instead of the local coverglass is a function –whose form is to be specified by the user- of the so-called reduced potential:

$$\Phi_{red} = -|q|/q\ (\Phi_{IC}-\Phi_{DIEL})/E$$

Model 2 takes advantage of this method too. As written in Table 1, model 2 uses Astrium's model A (see Figure 13) to calculate the ratio of current collected by the IC. The model is as follows, for an electron: $\Phi_{RED}>>1$ means 1/ that IC's potential is much more positive than coverglass' potential so that electric field lines in IC's vicinity define a potential well surrounding the IC; and 2/ that electron's kinetic energy is negligible with respect to the force of the potential well such that the particle falls in the potential well and is collected by the IC. Hence, ICs collection ratio is 1 when $\Phi_{RED}>>1$. Given that ICs are very small compared to coverglass surface, $\Phi_{RED}<0$ means that coverglass potential is equal or more positive than IC's potential so IC's collection ratio is 0: all electrons are collected by coverglass. To simplify the function, a linear form has arbitrarily been chosen in the region $0<\Phi_{RED}<X$ where X is the minimum value of Φ_{RED} for which the IC's ratio is 1. In conclusion, model A has X as the unique tuning parameter.

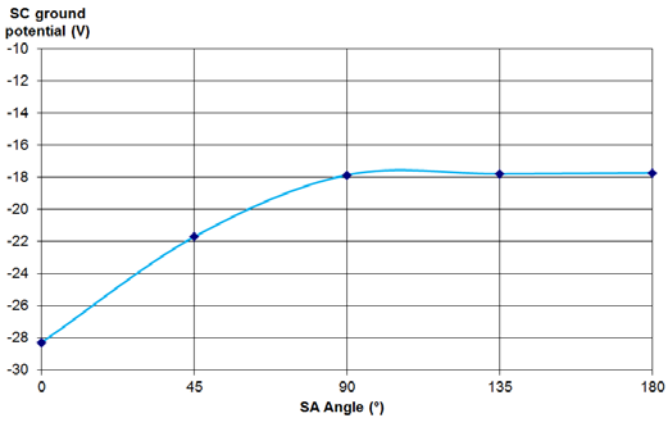

Figure 16: Model-2-predicted potential vs SA angle.

Model 2 results: Figure 16 shows the SMART-1 ground's potential obtained with model 2 at different SA angles. The result for 180° is the same because ICs do not play any role. On the contrary, the potential at 0° is lower, -28 V instead of -35 V. The potential excursion for a 180° rotation is thus 10 V instead of 17 V for model 1. This is a direct consequence of limiting IC-collected electron current by assuming them to be within the coverglass sheath instead of draining electrons directly from the undisturbed plume plasma.

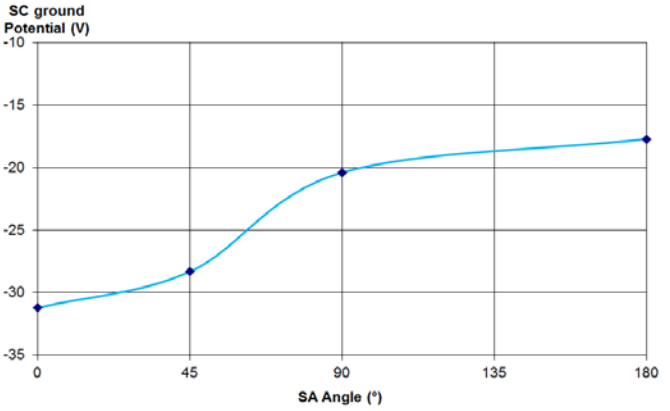

Figure 17: Model-3-predicted potential vs SA angle.

Model 3 description: model 3 includes the 6 solar panels instead of just 1 like in models 1 and 2.

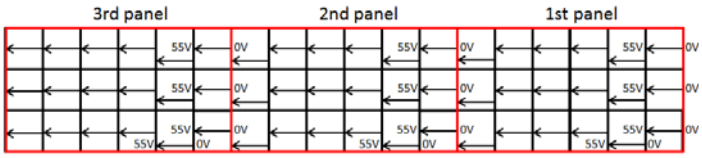

Figure 18: Detailed IC potential distribution.

Model 3 results: Figure 17 shows that, when solar cells and ICs are on plume's side (0°), ground's potential goes more negative than with model 2. The reason is that IC-collected electron current, which directly accounts in ground's electrical balance, is around 6 times higher. Total ion current on the panel is also around 6 times higher but, being collected by coverglass, it does not reach SC's ground.

Model 4 description: with regard to models 2 and 3, IC's potential and geometrical description in model 4 is much closer to real SMART-1's configuration (see Figure 18). IC's potential increases linearly between V_{ground}

and V_{ground}+55 V: each rectangle corresponds to a string of 33 solar cells. In models 1, 2 and 3, all ICs were assumed to be at V_{ground}+55 V for simplicity.

Model 4 results: model 4 predicts -17.7 V at 180°, just like all other models, and -18.3 V at 0° instead of -32 V for model 3 and -28 V for model 2. This means an excursion of only ~1 V for a 180° rotation, which is very small compared to previous models and flight experience. This is the symptom that the ICs' effect is now underestimated. The large reduction of electron current collected by ICs is due to a too coarse mesh over the panel, which leads us to model 5.

Model 5 description: in model 5, the mesh size over solar panels is 4 times smaller than in models 1 to 4.

Model 5 results: because local ICs potentials influence ion and electron collection distribution between ICs and coverglass, they are expected to influence not only SC potential but also coverglass equilibrium potentials. Figure 19 shows that a refined mesh (mode 5 - right) allows the coverglass potentials to periodically increase and decrease in accordance to ICs' potential distribution (see Figure 18). Model 4 (left) fails to capture this phenomenon. The model shows that coverglass potential is more positive where ICs' potential is more negative and vice-versa.

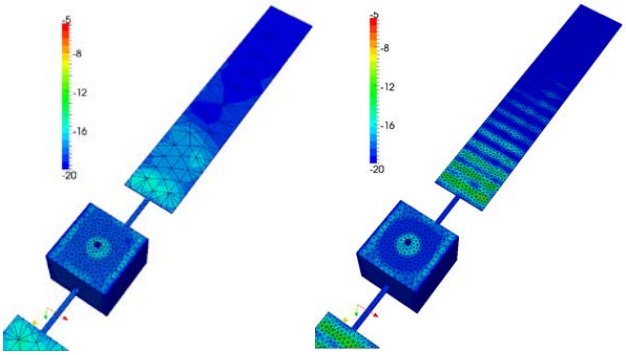

Figure 19: Coverglass potentials for coarse mesh (model 4) and refined mesh (model 5).

And yet, the SC ground potential obtained at 0° with model 5, -19 V, is more positive than expected. This conducted us to model 6.

Model 6 description: now that the solar array model has been enriched in terms of ICs' potential and geometrical description, number of panels and mesh, the last step was to use in-flight experimental data to tune the ICs' collection ratio model in order to obtain a 6 V excursion for a 180° rotation of the SA. The new model is called model B in Figure 13.

Model 6 results: Figure 20 shows the time evolution of potentials with model 6 for a SA at 0°. Thanks to model B, the obtained SC ground potential excursion for a 180° rotation of the SA is 6.8 V, which is sufficiently close to the ~6 V observed in flight.

Figure 21 shows the net currents collected by SC's ground, ICs and the SA (IC + coverglass). The ground collects a net current of 0.17 A, i.e. more ions than electrons. This current is mainly balanced by the net current collected by IC, -0.16 A, which collect large amounts of electrons. The remaining 0.01 A is the leak current through dielectric coatings: coverglass and MLI. The net currents on SA and ICs are identical, meaning that the net current on the coverglass is null.

This IC's collection ratio model shall be taken very cautiously as it has simply been tuned with SMART-1 data and it strongly depends on the electron temperature model used for plume modelling. By presenting the model here, our focus is more on the method that on the precise form of the function.

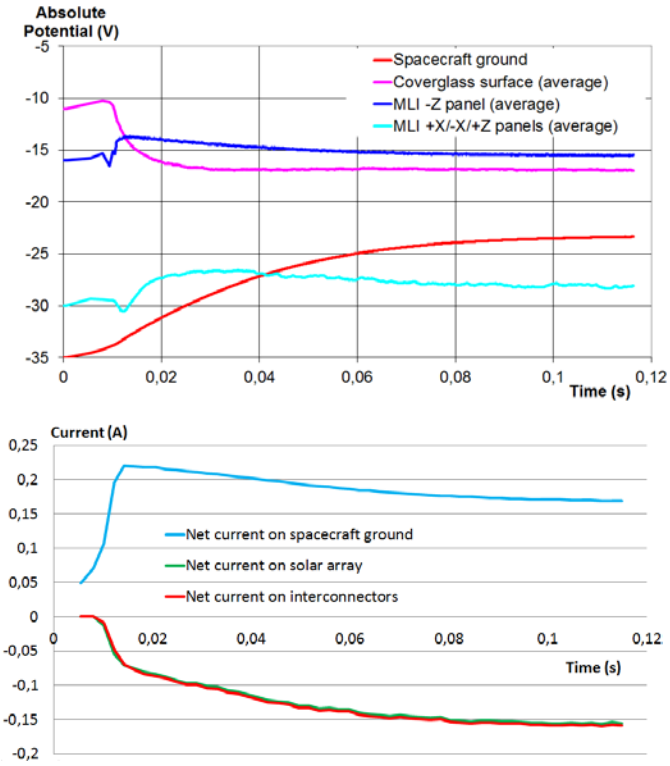

Figure 21: Currents at 0° - model 6.

IV. Ways Forward

SPIS has been added to the set of tools used by Astrium to simulate electric propulsion plume effects on the satellite. The tool is currently used in operational projects to perform detailed erosion analyses like in Figure 22. As mentioned in §II.A, HET-type plume models are currently being improved. Moreover, the complexity of plasma physics is such that improvement in several areas remains to be explored: this is for example the case of electrons modelling and cooling, the physical modelling of the plume in the near field or cathode simulation.

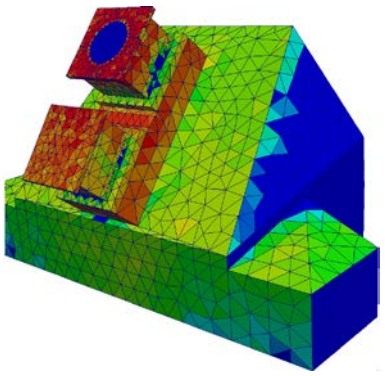

Figure 22: Erosion analysis with SPIS.

V. Conclusion

Plume models for different electric thrusters have been implemented in SPIS, tuned and validated. Also, a simple method has been developed in order to use SPIS for prediction of SC charging taking into account neutraliser's characteristic I-V curve. The method has been validated with a dedicated test performed at ESA premises. Finally, a simulation model of SMART-1 has been created in SPIS and tuned with flight data. The model is able to reproduce the effect on SC ground potential of solar cells' interconnectors and daily solar array rotation.

Acknowledgements

This work has been carried out with Eric Gengembre, Technical Officer of the ESA contract N. 22730/09/NL/SFe.

References

[1] Wartelski, M. et al., *The Assessment of Interactions between SC and Electric Propulsion Systems Project*, 32nd IEPC, October 2011, Wiesbaden, IEPC-2011-028.

[2] Bulit, A. et al., *Experimental Investigation on the Influence of the Facility Background Pressure on the Plume of the RIT-4 Ion Engine*, 32nd IEPC, October 2011, Wiesbaden, IEPC-2011-014.

[3] Wartelski, M. et al., *Simulation of Interactions Between SC and Electric Thrusters Using the SPIS tool*, 3rd ISPC, May 2012, Bordeaux, SP2012-2364082.

[4] C. Koppel et al., *The SMART-1 Hall Effect Thruster Around the Moon: In Flight Experience*, 29th IEPC, Princeton, November 2005, IEPC-2005-119.

[5] Hilgers et al., *A Simple Model of the Effect of SA Orientation on SMART-1Floating Potential*, IEEE Transactions on Plasma Science, Vol. 34, No. 5, October 2006.

[6] D. Estublier., *SMART-1 SC Potential Investigations*, IEEE Transactions on Plasma Science, Vol. 36, NO. 5, October 2008.

[7] M. Tajmar et al., *Numerical Simulation of SMART-1 Hall-Thruster Plasma Interactions*, Journal of Propulsion and Power, Vol 25, Issue 6, November-December 2009.